Spin splitting in a MoS_2 monolayer induced by exciton interaction

Yao Li,[1] Guangyao Li,[2,3,*] Xiaokun Zhai,[4] Shifu Xiong,[4] Hongjun Liu,[4] Xiao Wang,[5] Haitao Chen,[6] Ying Gao,[1] Xiu Zhang,[1] Tong Liu,[7] Yuan Ren,[7] Xuekai Ma,[8] Hongbing Fu,[1] and Tingge Gao[1,†]

[1]*Tianjin Key Laboratory of Molecular Optoelectronic Science, Institute of Molecular Plus, School of Science, Tianjin University, Tianjin 300072, China*

[2]*School of Physics and Astronomy, Monash University, Victoria 3800, Australia*

[3]*ARC Centre of Excellence in Future Low-Energy Electronics Technologies, Monash University, Victoria 3800, Australia*

[4]*Institute of Functional Crystals, Tianjin University of Technology, Tianjin 300384, China*

[5]*Key Laboratory for Micro-Nano Physics and Technology of Hunan Province, School of Physics and Electronics, Hunan University, Changsha, Hunan 410012, China*

[6]*College of Advanced Interdisciplinary Studies, National University of Defence Technology, Changsha, Hunan 410073, China*

[7]*Department of Aerospace Science and Technology, Space Engineering University, Beijing 101416, China*

[8]*Department of Physics and Center for Optoelectronics and Photonics Paderborn (CeOPP), Universität Paderborn, Warburger Strasse 100, 33098 Paderborn, Germany*

(Received 6 January 2020; revised manuscript received 25 May 2020; accepted 28 May 2020; published 25 June 2020)

By pumping nonresonantly a MoS_2 monolayer at 13 K under a circularly polarized continuous wave (CW) laser, we observe exciton energy redshifts that break the degeneracy between B excitons with opposite spin. The energy splitting increases monotonically with the laser power reaching as much as 18 meV, and it diminishes with the increase of temperature. The phenomenon can be explained theoretically by considering simultaneously the band-gap renormalization that gives rise to the redshift and exciton-exciton Coulomb exchange interaction that is responsible for the spin-dependent splitting. Our results offer a simple scheme to control the valley degree of freedom for MoS_2 monolayers and provide an accessible method in investigating the many-body exciton-exciton interaction in such materials.

DOI: 10.1103/PhysRevB.101.245439

I. INTRODUCTION

Transition metal dichalcogenides (TMDs) attracted great attention recently because of their unique photonic and optoelectronic properties [1–3]. When a bulk TMD is thinned down to a monolayer (ML), it becomes a direct band-gap material with gaps located at K and K' points [4,5] in the corners of the Brillouin zone. Owning to the spin-orbit interactions, each valley is spin-split, resulting in two distinct exciton resonances denoted as A and B excitons [5,6]. TMD excitons' binding energy (about 0.5 eV) is much larger than that of GaAs (10 meV), with a smaller Bohr radius a_B (1 nm *vs* 10 nm), so that their excitonic features are robust even at room temperature [3], and providing a solid platform to investigate exciton physics over a broad range of temperature and excitation density [7–9]. Since the states in the K and K' valley are related with each other by time-reversal symmetry, the corresponding exciton energies of the same type from different valley are degenerate [4,10,11]. In the interest of engineering TMD based valleytronic devices, it is desirable to lift the energy degeneracy to make use of the valley degree of freedom [12]. In experiments, it has been demonstrated that the exciton degeneracy can be broken by an out-of-plane magnetic field up to 10 T [13–19]. Such apparatus, however, might not be applicable in realistic applications.

Another experimentally accessible method to lift the degeneracy is by employing the optical Stark effect [20,21]. When a pulsed laser pumps the TMD ML with energy just below the exciton resonance, the hybridization between the equilibrium state and the photon-dressed state will shift the exciton energy to a higher value. By applying a pulsed probe laser to measure the change of absorption or reflection spectra, the exciton energy degeneracy between different valleys can be lifted if the pump laser is circularly polarized [20,21], which is supposedly equivalent to a 60-T pseudomagnetic field for a 10-meV splitting. This approach, however, not only requires a very high laser power density (Gigawatt/cm^2), but also it is intrinsically transient, which can only reveal a TMD ML's dynamical properties within the pump pulse duration. Therefore, an optically tunable exciton splitting scheme applicable to a quasiequilibrium scenario in the TMD ML is still missing.

In this work, we demonstrate experimentally that the energy degeneracy of excitons of the same type of different valley in a MoS_2 ML can be broken by the spin-dependent exciton-exciton interactions via a circularly polarized CW pump at 13 K. In experiments, with a nonresonant (2.33 eV) pump laser, we observed notable energy splitting for B excitons in the MoS_2 ML sample, where the splitting amount can be tuned continuously from 0 to 18 meV by changing

*guangyao.li@monash.edu
†tinggegao@tju.edu.cn

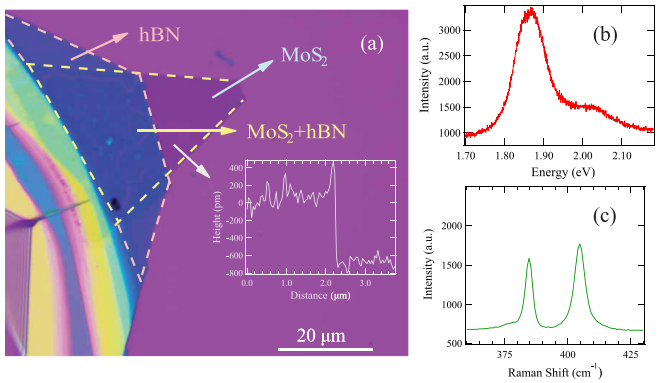

FIG. 1. Optical characterization of the sample. (a) The optical image and the AFM mapping of the MoS_2 ML, where the inset shows the thickness of the sample is about 0.7 nm. (b) PL spectrum of the MoS_2 ML excited by a 532-nm laser at room temperature. (c) Raman spectrum of the sample at room temperature.

the pumping power. Meanwhile, the splitting of A excitons and trions are very small because they have a smaller valley polarization. Theoretically, the splitting results from the disagreement of exciton-exciton interaction between different valleys, which raises the exciton energies differently [22], on top of an overall band gap renormalization given by free carriers [23,24]. Our results offer a different way to control the valley degree of freedom, and could be directly applicable to TMD ML exciton-polariton systems [25,26].

II. EXPERIMENTAL DETAILS

A piece of MoS_2 ML is grown at 760 K by the chemical vapor deposition (CVD) on a SiO_2/Si substrate. To protect the ML, a hexagonal boron nitride (hBN) layer with thickness of around 10 nm is transferred on top of the sample, as shown in the atomic force microscopy (AFM) characterization in Fig. 1(a). We measured the optical spectrum of the MoS_2 ML by a home-built confocal photoluminescence setup, see Supplemental Material (SM) for details [27], and obtained smooth photoluminescence spectra originated from the recombination of A excitons (1.865 eV) and B excitons (2.024 eV), as shown in Fig. 1(b). The 0.159 eV energy difference between A and B excitons agrees with previous measurements [28,29]. Figure 1(c) shows the Raman spectrum measured at room temperature by a commercial Raman microscope (WITec alfa 300), and the peak at 384.67 cm^{-1} confirms the good quality of the MoS_2 ML [30].

To study exciton-exciton interactions, the sample is cooled down to 13 K by a cryogen free cryostat (Janis). We use a 532-nm laser (Spectra Physics) as the excitation source. The laser can be adjusted from linear to circular (left- or right-handed) polarization by using a quarter wave plate. The laser is focused on the sample through an objective with a spot of around 2 μm, and the emitted photons are collected by the same objective. A quarter wave plate, half wave plate, and a linear polarizer are combined to resolve the polarization of the emitted photoluminescence from the sample. The polarization of photons is calculated by $P = (I^+ - I^-)/(I^+ + I^-)$, where

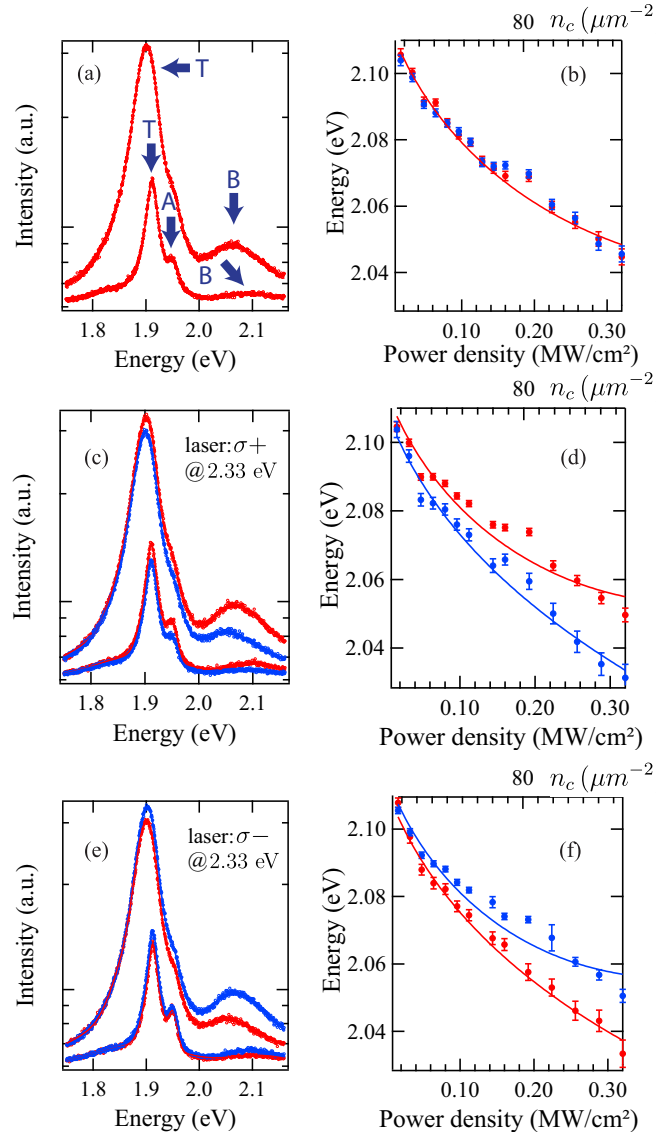

FIG. 2. The spectrum of the MoS_2 monolayer as a function of the pumping power. (a),(c),(e) Optical spectrum of the sample pumped by a linearly polarized, right-handed circularly polarized, and left-handed circularly polarized laser, respectively, with density of 0.016 MW/cm^2 and 0.192 MW/cm^2. The experimental data is shown by circles, the fitting cures are shown using lines. (b),(d),(f) PL peaks (fitted B exciton energy) against the pumping power density (bottom axis), with polarization matching the corresponding spectra on the left columns. Red (blue) dots correspond to B excitons at the K and K' valley, respectively. Solid curves are the theoretical plots against n_c (top axis) according to Eq. (4). Theory parameters can be found in Ref. [39].

I^+ and I^- denote the counts of the right- and left-handed circularly polarization components, respectively.

At 13 K, the energies of A and B excitons are blueshifted to 1.948 eV and 2.099 eV, respectively, and the trion peak appears at 1.911 eV [31] under the pump power density of 0.016 MW/cm^2, see Fig. 2(a). During the experiment, a mechanical chopper with a duty circle of 5% is used to reduce possible heating effect by the laser. When the pump power is continuously increased, the spectrum peaks

corresponding to exciton energies smoothly shift to lower values, i.e., redshifted, see Fig. 2(b). Previous experiments with similar pump power density have precluded the laser heating from being the cause of such an effect [32,33]. Similar exciton energy redshift has been reported previously in Ref. [9], where the anomalous redshift-blueshift crossover was measured by a pump-probe spectroscopy with a WS_2 ML and it was interpreted phenomenologically by a Lennard-Jones potential between excitons [9]. In our current experiment, we did not observe the redshift-blueshift crossover.

Next we discuss the exciton energy changes with the spin degrees of freedom. Since the A exciton peak overlaps with the trion peak [31] and it was demonstrated previously that the valley polarization effect of B excitons is much stronger than that of A excitons and trions [29], resulting in no observable spin splitting effect for the latter two resonances, here we focus on B excitons and sometimes refer them simply as excitons. Figure 2(c) shows the PL spectra of the MoS_2 ML pumped by a right-handed circularly polarized laser. The nonzero left-handed polarized PL is presumably caused by intervalley scattering [21], and the polarization P of B excitons is about 30%, which is in agreement with Ref. [29]. By examining the spectral peak positions of each polarization component, we find an energy splitting about 18 meV under the pump power of $0.32\,\mathrm{MW/cm^2}$. The energy splitting is reversed when the pump switches to the opposite polarization, see Fig. 2(e). In both cases, the energy of the copolarized component is always higher than that of the cross-polarized component, which is in contrast with the results of $MoSe_2/WSe_2$ heterostructures [34]. When the pump laser is linearly polarized, the splitting between two circular polarization components disappears, see Figs. 2(a) and 2(b).

III. RESULTS AND DISCUSSIONS

The spin dependent energy splitting can be explained by the exciton-exciton interaction originated from the Coulomb interaction between electrons and holes. Simply speaking, the population imbalance between B excitons in different valley gives rise to a different energy correction because of the Coulomb interaction. Similar splitting can also be found in conventional semiconductor quantum well systems such as GaAs or InAs [22,35–38]. However, the spin splitting observed previously was created under pulsed excitation and greatly reduced when the laser was tuned far away from the exciton resonance [36]. In our experiments, thanks to the spin-valley-locking mechanism, the laser energy to induce the exciton splitting can be much larger, which is 230-meV higher than the exciton resonance in MoS_2 ML, this leaves greater flexibility for the laser choice to control the valley degrees of freedom.

Compared with the optical Stark effect [20,21] in the TMDs ML, the exciton splitting can be manipulated under much lower pumping density. In the SM, we plot the exciton splitting as a function of the pumping density. The exciton splitting reaches 18 meV at the pumping density of around $0.32\,\mathrm{MW/cm^2}$, which is around four orders of magnitude smaller than that of the optical Stark effect [21]. In addition, we can tune the exciton splitting from zero to 18 meV continuously, which cannot be realized in Ref. [34]. Thus, the interexcitonic exchange interaction offers to tune the exciton splitting more effectively and stably in MoS_2 ML. In the following we develop a theory to model the energy splitting of the MoS_2 ML under various pumping configurations.

The measured exciton PL peak energy E^{PL}, which corresponds to the recombination of an electron in the conduction band with its paired hole in the valence band, can be expressed as

$$E^{PL} = E_g + (-E_B), \tag{1}$$

where E_g is the band gap and $-E_B$ is the exciton ground state binding energy (assuming the exciton is at rest). Equation (1) is the single-particle energy without any screening effect. When the pumping power increases, screening of the Coulomb potential due to excessive free carriers will change both the value of E_g and $-E_B$ simultaneously. The screening effect on E_g is called band-gap renormalization, which causes the overall redshift [40], while the screening effect on $-E_B$ causes energy blueshift. These two effects occur together and cannot be discriminated easily [32]. In the CW pumping regime, additionally, exciton-exciton interaction can become prominent, which also generates blueshift [35]. The competition between these three effects can give rise to interesting phenomenon such as redshift-blueshift crossover recently observed in experiments [9]. In the following, we will discuss phenomenologically how those energies change against the free carrier density n_c.

First we look at the band-gap renormalization (BGR). Intuitively, a reduced Coulomb interaction would change a quasiparticle's response to changes of its environment caused by the quasiparticle itself. This response is called self-energy [23]. The BGR can be calculated by looking at how the self-energy changes under the screened Coulomb potential. Following Ref. [23,24], the BGR after taking the random phase approximation and quasi-static approximation can be expressed as

$$\Delta E_g(n_c) = V_s(k_F)\, n_c + \sum_{\mathbf{q}} [V_s(\mathbf{q}) - V(\mathbf{q})], \tag{2}$$

where $V_s(\mathbf{q})$ and $V(\mathbf{q})$ are the screened and unscreened Coulomb potentials, respectively, and $k_F = (2\pi n_c)^{1/2}$ is the $2D$ Fermi wave number. On the right-hand side of Eq. (2), the first term is called a screened exchange, which corresponds to the change in electron occupation [41], and the second term is called the Coulomb-hole contribution, which is the difference in self-interaction between the screened and the unscreened Coulomb potential [24]. These two terms are widely used in the dynamically screened Coulomb interaction approximation also known as GW approximation [42]. Calculation details of $\Delta E_g(n_c)$ and the analytic expression of $V_s(\mathbf{q})$ can be found in the SM. Note that the BGR is shared between two valleys and it does not break the time-reversal symmetry.

Next we look at exciton binding energy screening and exciton-exciton interaction as functions of n_c. Owing to screening, the exciton binding energy will reduce to $-E_B/\varepsilon_r^2$ [43], with $\varepsilon_r(n_c)$ representing the modified dielectric constant. In the presence of valley degrees of freedom, if we ignore the Coulomb exchange between excitons from different valleys (equivalent to setting the excitons' center-of-mass momentum

to zero [44]), the meanfield first-order exciton-exciton interaction energy correction is: $\Delta E_\sigma^X \propto E_B n_\sigma^X$ [22], where n_σ^X is the excition density and $\sigma = \pm$ is the pump beam polarization index. Since we are away from the Mott transition, n_σ^X should be small (dilute) so that it can be expanded around $n_c = 0$ up to the quadratic term as $n_\sigma^X = a_\sigma + b_\sigma n_c^2$, where the linear term is omitted to avoid overfitting [45]. By applying similar expansion to $-1/\varepsilon_r^2$, we can combine the n_c-independent terms and the n_c^2 coefficients as s_σ and f_σ, respectively. Thus, we obtain the screened exciton energy correction:

$$\Delta E_\sigma^X(n_c) = \left(s_\sigma + f_\sigma\, n_c^2\right) E_B, \tag{3}$$

where s_σ and $f_\sigma > 0$ are fitting parameters. Combining Eqs. (1),(2), and (3), we can express the PL peak energy for excitons from different valleys as

$$E_\sigma^{PL}(n_c) = E_g + \Delta E_g(n_c) + \left(s_\sigma + f_\sigma\, n_c^2\right) E_B. \tag{4}$$

Figure 2 shows that the theoretical curves fit nicely to the experimental data across various pump beam polarizations. The n_c axis at the top and the power density axis at the bottom is connected through the shared energy axis, thus establishing a relationship between the two, which allows us to estimate the otherwise not measurable free carrier density in our system. Note that if we extend the theoretical plot of Eq. (4) beyond the current experimental range, the PL peak will exhibit redshift-blueshift crossover behavior when the energy correction term $f_\sigma\, n_c^2$ surpasses the other terms. In this case, however, the mean-field first-order perturbation theory will break down and a more rigorous calculation would be required. Nevertheless, based on the existing experimental data we can see that the nonlinear dependence of n_X on n_c could be responsible for the proposed Lennard-Jones -type potential in real space [9].

Our experimental results can be repeated in other MoS_2 samples using different fabrication techniques. In the SM, we show the existence of the spin splitting in a CVD grown MoS_2 monolayer without any hBN capping and in a mechanically exfoliated MoS_2 monolayer. Although the exciton energy and the doping density in those samples vary piece by piece, the spin splitting does not change too much under the same pumping condition. The splitting can especially be observed across various samples (see the SM for more details). This rules out the possibility that the spin splitting is a result of interaction with the capping hBN layer or with defects inherited from the growth process. In addition, the spin splitting also exists in a MoS_2 monolayer using a pure silicon and hBN substrate (shown in SM), excluding effects from the substrate.

With increasing the temperature, both A and B excitons will shift to lower energies. In Fig. 3, we repeated the measurements at different temperatures (15, 50, 100, 150, 200, 250, and 300 K). At higher temperature, the circular polarization of the photoluminescence decreases due to the phonon-assisted intervalley scattering, in agreement with Refs. [29,46–48]. Although the spectra corresponding to the B exciton can keep the circular polarization even at room temperature (10%), The spin splitting under the circularly polarized pumping approaches zero at around 200 K, as shown in Fig. 3(b) and 3(d).

The band-gap renormalization and exciton intervalley relaxation dynamics have been investigated extensively by

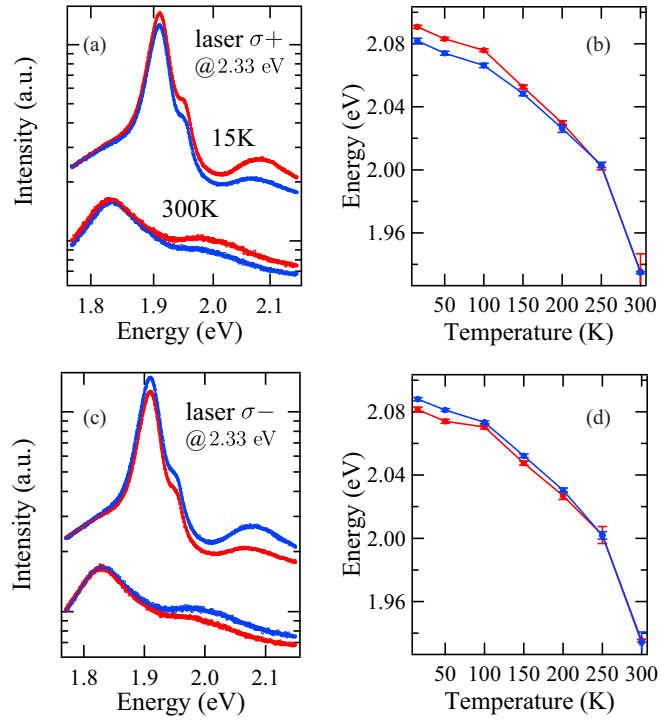

FIG. 3. PL spectra of the MoS_2 ML at different temperatures. (a),(c) Optical spectra at 15 and 300 K pumped by a right- and left-handed circularly polarized laser, respectively. The experimental data is shown by circles, the fitting curves are shown using lines. Power density: 0.048 MW/cm^2. (b),(d) Exciton energy against temperature.

pump-probe experiments [32,49–51], where the fast intervalley scattering helps populate the unpumped valley, thus reducing the valley polarization. These processes happen at a time scale of a few picoseconds. In our experiments, since the CW pump duration is much longer than the time scales of those relaxation processes, dynamical equilibrium can be assumed to be reached, i.e., the system is in a steady state. This explains why our use of previously established quasiequilibrium theory can fit the experimental data so well.

IV. SUMMARY

We show experimentally and theoretically that spin dependent exciton-exciton interaction under a circularly polarized pump can lead to exciton energy splitting between different valleys in a MoS_2 ML. The spin splitting can be tuned up to 18 meV at a relatively low power density (MW/cm^2), which is much more efficient than the optical Stark effect. In addition, it does not need an external magnetic field or stacking of different materials. The CW-pumping-created spin splitting provides a reliable way to explore the valley degrees of freedom for MoS_2 ML systems and it is readily applicable to the investigation of the spin dynamics of TMD exciton-polaritons.

ACKNOWLEDGMENTS

T.G. acknowledges the support from the National Natural Science Foundation of China (No. 11874278), H.L. thanks for the support from the National Natural Science

Foundation of China (No. 51672076), H.C. and X.M. acknowledge the National Natural Science Foundation of China (No. 11804387, No. 11804064), respectively. G.L. thanks Dr. D.y Efimkin and Dr. B. Hopkins for useful discussions. T.G, Y.L. thank Yunan Gao and Yunkun Wang for the help during the sample preparation.

[1] X. Xu, W. Yao, D. Xiao, and T. F. Heinz, Nat. Phys. **10**, 343 (2014).
[2] Q. H. Wang, K. Kalantar-Zadeh, A. Kis, J. N. Coleman, and M. S. Strano, Nat. Nanotechnol. **7**, 699 (2012).
[3] G. Wang, A. Chernikov, M. M. Glazov, T. F. Heinz, X. Marie, T. Amand, and B. Urbaszek, Rev. Mod. Phys. **90**, 021001 (2018).
[4] A. Splendiani, L. Sun, Y. Zhang, T. Li, J. Kim, C.-Y. Chim, G. Galli, and F. Wang, Nano Lett. **10**, 1271 (2010).
[5] K. F. Mak, C. Lee, J. Hone, J. Shan, and T. F. Heinz, Phys. Rev. Lett. **105**, 136805 (2010).
[6] T. Mueller and E. Malic, Npj 2D Mater. Appl. **2**, 29 (2018).
[7] A. Chernikov, C. Ruppert, H. M. Hill, A. F. Rigosi, and T. F. Heinz, Nat. Photon. **9**, 466 (2015).
[8] G. Aivazian, H. Yu, S. Wu, J. Yan, D. G. Mandrus, D. Cobden, W. Yao, and X. Xu, 2D Materials **4**, 025024 (2017).
[9] E. J. Sie, A. Steinhoff, C. Gies, C. H. Lui, Q. Ma, M. Rösner, G. Schönhoff, F. Jahnke, T. O. Wehling, Y.-H. Lee, J. Kong, P. Jarillo-Herrero, and N. Gedik, Nano Lett. **17**, 4210 (2017).
[10] D. Xiao, G.-B. Liu, W. Feng, X. Xu, and W. Yao, Phys. Rev. Lett. **108**, 196802 (2012).
[11] G.-B. Liu, W.-Y. Shan, Y. Yao, W. Yao, and D. Xiao, Phys. Rev. B **88**, 085433 (2013).
[12] J. R. Schaibley, H. Yu, G. Clark, P. Rivera, J. S. Ross, K. L. Seyler, W. Yao, and X. Xu, Nat. Rev. Mater. **1**, 16055 (2016).
[13] Y. Li, J. Ludwig, T. Low, A. Chernikov, X. Cui, G. Arefe, Y. D. Kim, A. M. van der Zande, A. Rigosi, H. M. Hill, S. H. Kim, J. Hone, Z. Li, D. Smirnov, and T. F. Heinz, Phys. Rev. Lett. **113**, 266804 (2014).
[14] A. Srivastava, M. Sidler, A. V. Allain, D. S. Lembke, A. Kis, and A. Imamoğlu, Nat. Phys. **11**, 141 (2015).
[15] D. MacNeill, C. Heikes, K. F. Mak, Z. Anderson, A. Kormányos, V. Zólyomi, J. Park, and D. C. Ralph, Phys. Rev. Lett. **114**, 037401 (2015).
[16] G. Aivazian, Z. Gong, A. M. Jones, R.-L. Chu, J. Yan, D. G. Mandrus, C. Zhang, D. Cobden, W. Yao, and X. Xu, Nat. Phys. **11**, 148 (2015).
[17] C. Zhao, T. Norden, P. Zhang, P. Zhao, Y. Cheng, F. Sun, J. P. Parry, P. Taheri, J. Wang, Y. Yang, T. Scrace, K. Kang, S. Yang, G.-X. Miao, R. Sabirianov, G. Kioseoglou, W. Huang, A. Petrou, and H. Zeng, Nat. Nanotechnol. **12**, 757 (2017).
[18] T. Norden, C. Zhao, P. Zhang, R. Sabirianov, A. Petrou, and H. Zeng, Nat. Commun. **10**, 4163 (2019).
[19] J. Zhang, L. Du, S. Feng, R.-W. Zhang, B. Cao, C. Zou, Y. Chen, M. Liao, B. Zhang, S. A. Yang, G. Zhang, and T. Yu, Nat. Commun. **10**, 4226 (2019).
[20] E. J. Sie, J. W. McIver, Y.-H. Lee, L. Fu, J. Kong, and N. Gedik, Nat. Mater. **14**, 290 (2015).
[21] J. Kim, X. Hong, C. Jin, S.-F. Shi, C.-Y. S. Chang, M.-H. Chiu, L.-J. Li, and F. Wang, Science **346**, 1205 (2014).
[22] J. Fernández-Rossier, C. Tejedor, L. Muñoz, and L. Viña, Phys. Rev. B **54**, 11582 (1996).
[23] H. Haug and S. Schmitt-Rink, Prog. Quant. Electron **9**, 3 (1984).
[24] C. Ell, R. Blank, S. Benner, and H. Haug, J. Opt. Soc. Am. B **6**, 2006 (1989).
[25] S. Wang, S. Li, T. Chervy, A. Shalabney, S. Azzini, E. Orgiu, J. A. Hutchison, C. Genet, P. Samorì, and T. W. Ebbesen, Nano Lett. **16**, 4368 (2016).
[26] X. Liu, T. Galfsky, Z. Sun, F. Xia, E. Lin, Y.-H. Lee, S. Kéna-Cohen, and V. M. Menon, Nat. Photon. **9**, 30 (2015).
[27] See Supplemental Material at http://link.aps.org/supplemental/10.1103/PhysRevB.101.245439 for details, which includes Refs. [54–58].
[28] K. F. Mak, K. He, J. Shan, and T. F. Heinz, Nat. Nanotechnol. **7**, 49 (2012).
[29] G. Sallen, L. Bouet, X. Marie, G. Wang, C. R. Zhu, W. P. Han, Y. Lu, P. H. Tan, T. Amand, B. L. Liu, and B. Urbaszek, Phys. Rev. B **86**, 081301(R) (2012).
[30] W. M. Parkin, A. Balan, L. Liang, P. M. Das, M. Lamparski, C. H. Naylor, J. A. Rodríguez-Manzo, A. T. C. Johnson, V. Meunier, and M. Drndić, ACS Nano **10**, 4134 (2016).
[31] J. W. Christopher, B. B. Goldberg, and A. K. Swan, Sci. Rep. **7**, 14062 (2017).
[32] F. Liu, M. E. Ziffer, K. R. Hansen, J. Wang, and X. Zhu, Phys. Rev. Lett. **122**, 246803 (2019).
[33] X. Fan, W. Zheng, H. Liu, X. Zhuang, P. Fan, Y. Gong, H. Li, X. Wu, Y. Jiang, X. Zhu, Q. Zhang, H. Zhou, W. Hu, X. Wang, X. Duanb, and A. Pan, Nanoscale **9**, 7235 (2017).
[34] C. Jiang, A. Rasmita, W. Xu, A. Imamoğlu, Q. Xiong, and W.-B. Gao, Phys. Rev. B **98**, 241410(R) (2018).
[35] L. Viña, L. Muñoz, E. Pérez, J. Fernández-Rossier, C. Tejedor, and K. Ploog, Phys. Rev. B **54**, R8317(R) (1996).
[36] Z. Sun, Z. Y. Xu, Y. Ji, B. Q. Sun, B. R. Wang, S. S. Huang, and H. Q. Ni, Appl. Phys. Lett. **90**, 071907 (2007).
[37] T. C. Damen, L. Viña, J. E. Cunningham, J. Shah, and L. J. Sham, Phys. Rev. Lett. **67**, 3432 (1991).
[38] P. Le Jeune, X. Marie, T. Amand, F. Romstad, F. Perez, J. Barrau, and M. Brousseau, Phys. Rev. B **58**, 4853 (1998).
[39] Theory parameters: $E_g = 2.15$ eV and $E_B = 0.44$ eV [3]; $\omega = 0$ (static screening); $\epsilon_0 = \epsilon_r\epsilon_0$ with $\epsilon_r = 4.47$ [52] and ϵ_0 the vacuum permittivity; $m_e = 0.53\ m_0$ and $m_h = 0.65\ m_0$ [53] with m_0 the free electron mass; Fig. 2(b): $s_\sigma = 6.43 \times 10^{-2}$ and $f_\sigma = 1.45 \times 10^{-6}\ \mu m^4$; Fig. 2(d): $s_+ = 6.67 \times 10^{-2}$, $f_+ = 2.22 \times 10^{-6}\ \mu m^4$ and $s_- = 5.42 \times 10^{-2}$, $f_- = 3.15 \times 10^{-9}\ \mu m^4$; Fig. 2(f) $s_+ = 5.84 \times 10^{-2}$, $f_+ = 2.77 \times 10^{-7}\ \mu m^4$ and $s_- = 6.62 \times 10^{-2}$, $f_- = 2.52 \times 10^{-6}\ \mu m^4$.
[40] F. T. Vasko and A. V. Kuznetsov, *Electronic States and Optical Transitions in Semiconductor Heterostructures*, (Springer, Berlin, 1999), Chap. 9.
[41] S. Gao and L. Yang, Phys. Rev. B **96**, 155410 (2017).
[42] L. Hedin, J. Phys. Condens. Matter **11**, R489 (1999).
[43] Monique Combescot and Shiue-Yuan Shiau, *Excitons and Cooper Pairs: Two Composite Bosons in Many-Body Physics* (Oxford University Press, Oxford, 2016).

[44] H. Yu, G. Bin Liu, P. Gong, X. Xu, and W. Yao, Nat. Commun. **5**, 3876 (2014).

[45] If n_σ^X is expanded only up to a linear term in n_c; , then the fitted coefficient of the linear term would be negative. Physically, it means that the exciton density decreases with the increase of free carrier density. This is unreasonable. If both the linear term and the quadratic term were included, then the experimental data would be overfitted. Therefore, the fitting expression of Eq. (3) is quadratic without a linear term.

[46] H. Zeng, J. Dai, W. Yao, D. Xiao, and X. Cui, Nat. Nanotechnol. **7**, 490 (2012)

[47] D. Lagarde, L. Bouet, X. Marie, C. R. Zhu, B. L. Liu, T. Amand, P. H. Tan, and B. Urbaszek, Phys. Rev. Lett. **112**, 047401 (2014)

[48] S. Wu, C. Huang, G. Aivazian, J. S. Ross, D. H. Cobden, and X. Xu, ACS Nano **7**, 2768 (2013).

[49] R. Schmidt, G. Berghäuser, R. Schneider, M. Selig, P. Tonndorf, E. Malić, A. Knorr, S. M. de Vasconcellos, and R. Bratschitsch, Nano Lett. **16**, 2945 (2016).

[50] M. Selig, F. Katsch, R. Schmidt, S. Michaelis de Vasconcellos, R. Bratschitsch, E. Malic, and A. Knorr, Phys. Rev. Res. **1**, 022007(R) (2019).

[51] G. Berghäuser, I. Bernal-Villamil, R. Schmidt, R. Schneider, I. Niehues, P. Erhart, S. M. de Vasconcellos, R. Bratschitsch, A. Knorr, and E. Malic, Nat. Commun. **9**, 971 (2018).

[52] G. Wang, I. C. Gerber, L. Bouet, D. Lagarde, A. Blocchi, M. Vidal, E. Palleau, T. Amand, X. Marie, and B. Urbaszek, 2D Mater. **2**, 045005 (2015).

[53] Z. Jin, X. Li, J. T. Mullen, and K. W. Kim, Phys. Rev. B **90**, 045422 (2014).

[54] J. Pandey and A. Soni, Appl. Surf. Sci. **463**, 52 (2019).

[55] F. Cadiz, E. Courtade, C. Robert, G. Wang, Y. Shen, H. Cai, T. Taniguchi, K. Watanabe, H. Carrere, D. Lagarde, M. Manca, T. Amand, P. Renucci, S. Tongay, X. Marie, and B. Urbaszek, Phys. Rev. X **7**, 021026 (2017).

[56] E. V. Calman, C. J. Dorow, M. M. Fogler, L. V. Butov, S. Hu, A. Mishchenko, and A. K. Geim, Appl. Phys. Lett. **108**, 101901 (2016).

[57] M. L. Trolle, T. G. Pedersen, and V. Véniard, Sci. Rep. **7**, 39844 (2017).

[58] A. Steinhoff, M. Rösner, F. Jahnke, T. O. Wehling, and C. Gies, Nano Lett. **7**, 3743 (2014).